Experimental Investigation of Evacuated Flat Plate Collector coupled with a Calorifier

Hamza Saeed[a,*], Abdul Haseeb[a], Adeel Waqas[a], Majid Ali[a], Hassan Nazir[a], Naveed Ahmed[a], Waqas Khalid[b], Zafar Said[c], Mariam Mahmood[a,*]

[a] *US-Pakistan Centre for Advanced Studies in Energy (USPCAS-E), National University of Sciences and Technology, Islamabad 44000, Pakistan*
[b] *School of Mechanical and Manufacturing Engineering, National University of Sciences and Technology, Islamabad 44000, Pakistan*
[c] *Department of Sustainable and Renewable Energy Engineering, University of Sharjah, United Arab Emirates*

Abstract

A global green transition is in progress to tap the renewable energy resources owing to the rising greenhouse gases and fluctuating fossil fuel prices around the world. Taking this into consideration, a small-scale evacuated flat plate solar thermal system is designed and installed to harvest solar energy for low temperature applications. This test rig consists of Evacuated Flat Plate Collectors (EFPCs) coupled with a helical coil calorifier. The helical coil acts as a heat exchanger between the heat transfer fluid and water within the calorifier. To evaluate the thermal performance, real-time experimentation is performed during the winter season, on the EFPC system under the outdoor climatic conditions at the US-Pakistan Center for Advanced Studies in Energy, NUST, Islamabad, Pakistan. The novelty of using a low vacuum pressure ~20 kPa hinders the convective thermal losses in EFPCs, thus the average daily thermal efficiency reaches a maximum value of 73%, with the glycol-water mixture as heat transfer fluid at a flow rate of 3 liters per minute. Moreover, the EFPC outlet temperature reaches a maximum value of 61 °C on a clear day during winters. Thus, an EFPC system can be used for hot water consumption as well as space heating applications.

Keywords: *Flat Plate Collector; Vacuum; Solar Energy; Performance Analysis*.

1. Introduction

Energy demand has been increased all over the world since the industrial revolution. The increase of human population and the need for the everchanging technologies has led to the rise of the energy demand. International Energy Agency (IEA) report of 2020 discloses that the Total Final Energy Consumption (TFEC) of the world in 1973 was 4,659 Mtoe which rose to 9,938 Mtoe in 2018 [1]. This increase in energy demand has led the scientists to work towards more eco-friendly and economical sources of energy instead of fossil fuels. The price hikes in the fuels sector is also a factor to shift towards green energy sources.

Solar energy is an abundant source of energy. Pakistan receives annual solar insolation of 1900-2200 kWh/m² which makes it quite a substantial potential for Pakistan to tap into solar energy [2]. Solar energy can be used to generate electricity as well as hot water to meet ever increasing demands of human population. The hot water can be used for space heating in homes during winters as well as in industry for process steam production. A target to reach to on grid share of 25% by renewable energy is set by Alternative Energy Development Board (AEDB) Pakistan [3]. Several different types of solar thermal collectors are being used to harvest solar energy. They can be categorized based on their surface areas, concentration ratios, types of heat transfer fluid used etc.

One of the applications of solar thermal collectors is their use for space heating and water heating. Solar thermal collectors are widely used during winters for water heating in homes as well as industrial applications. A basic Flat plate collectors (FPC) consists of a dark-colored metallic sheet absorber to absorb the incident solar radiation. The absorber is covered by a transparent sheet of glass or plastic. Copper tubes are connected to the absorber. Dagdougui et al. investigated the thermal efficiency of a flat plate collector using different types of covers for the location of Tetouan and Morocco. Increasing the number of plexiglass covers on the absorber results in decreasing the top heat loss coefficient (Ut) [4]. A simple flat plate collector has good optical performance but their thermal performance decreases with the rise in absorber temperature [5].

In an Evacuated Tube Solar Collector (ETC), the metallic absorber tube is covered with two concentric glass tubes. The space between tubes is sealed and evacuated. The inner absorber tube is usually coated with black paint to gain maximum

*Corresponding author. (1) M. Mahmood
Tel.: +92 5190855296; fax: NA
E-mail address: mariam@uspcase.nust.edu.pk
*Corresponding author. (2) H. Saeed
E-mail address: msaeedese18.ces@student.nust.edu.pk

incident solar energy. This evacuated space hampers the thermal convective losses. At lower temperatures, ETCs have much higher efficiency. Under the same climatic conditions, a simple ETC generates 9% more thermal energy than a FPC [6].

An evacuated flat plate collector (EFPC) combines a FPC and an ETC. The evacuated flat plate collector provides the combined positive aspects of the FPC and an ETC [5]. In EFPC, air is pumped out using a vacuum pump to minimize convective thermal losses. It combines the positive aspects of a simple FPC and ETC to harvest maximum solar energy. The purpose of this research study involves the experimental analysis and evaluation of an evacuated flat plate collector system under low vacuum conditions. A small scale EFPC system is designed and installed. Several experiments are performed by varying flow rates under ambient conditions during winters. The present study is performed for the location USPCAS-E, NUST under the climatic conditions of Islamabad, Pakistan.

2. Experimental Setup

2.1. Procedure

A small scale, active and closed loop evacuated flat plate collector system coupled with a calorifier is installed on the roof of US-Pakistan Centre for Advanced Studies in Energy (USPCASE), National University of Sciences and Technology (NUST), Islamabad, Pakistan.

The system consists of 2 EFPC panels, a solar controller, a circulator, an expansion vessel, and a helical coil calorifier. EFPCs are installed at a tilt angle of 30° facing South. The heat transfer fluid used is a mixture of Glycol and Water. The controller is used to run the HTF through piping system and the EFPC panels. The HTF absorbs heat from the EFPC absorber and delivers it to the water in the calorifier. The calorifier installed is a helical coil heat exchanger with water storage which transfers heat from primary loop to the secondary loop. The helical coil is made of copper while the tank is fabricated using galvanized iron sheets. The secondary loop is simply the calorifier filled with water for domestic hot water consumption.

The EFPCs are connected in such a way that the pipes from the calorifier to the collector and from the collector to the calorifier are equal in length. This is known as Tichelmann configuration. This configuration ensures the uniform flow rate and uniform heating of the HTF without the use of control valves. The flow rate is controlled using a flow meter. The pressure in the piping system is kept at 2 bar during circuit filling. An expansion vessel is also installed in the system to cope with the fluctuations in HTF pressure during heating and cooling of the fluid. Complete schematic diagram is shown in Fig 1.

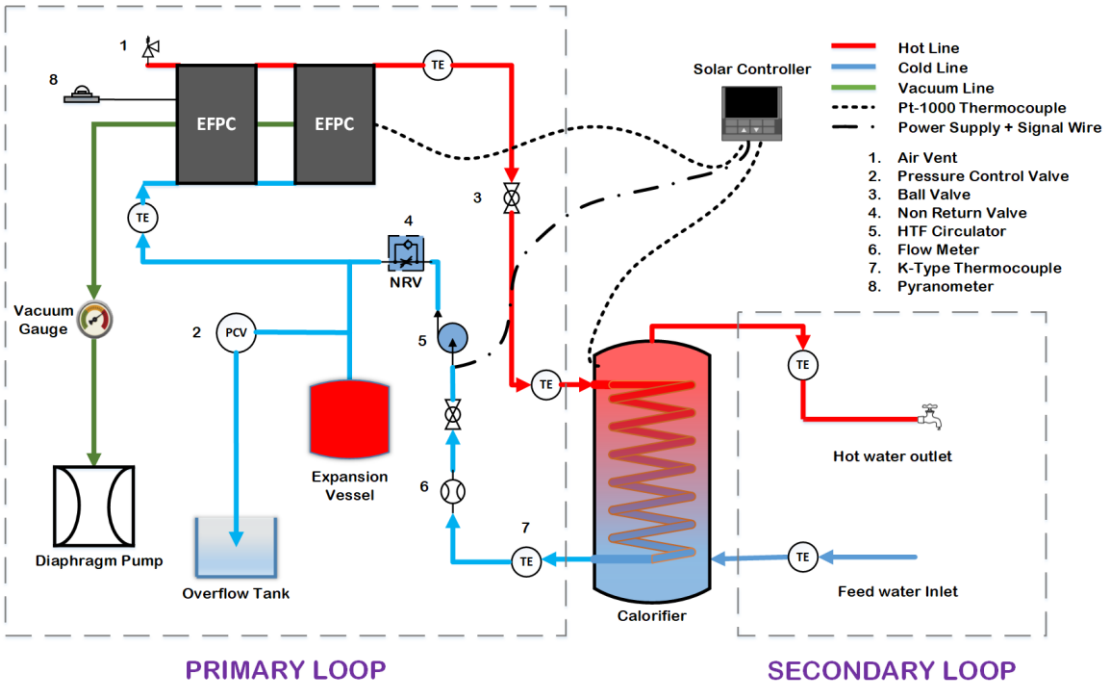

Fig. 1: Schematic Diagram of EFPC experimental system.

A vacuum diaphragm pump is used for the evacuation of the EFPC panels. The vacuum pump can reduce the pressure from 101.325 kPa to a minimum value of 20.0 kPa inside the EFPC panels. This enables a substantial decrease in the convective losses.
The controller installed controls the working of the circulator based on the temperatures of Pt-1000 thermocouples installed at the EFPC panel and the storage tank. A higher difference between the two thermocouples makes the circulator run while it stops when the temperature of the two thermocouples is in equilibrium.

Fig. 2: EFPC system with calorifier, expansion vessel, data logger and control unit in the background

The entire primary and secondary circuits are also installed with several thermocouples to study heat losses and temperature of HTF/water at various inlets and outlets to calculate useful energy as shown in Fig 2. A rotameter is also installed in the primary circuit to control volume flow rate depending on site-specific conditions as well as test conditions.

2.2. Calculations

To find the overall efficiency of the EFPC system, a thermal resistance network is required to calculate the overall heat loss coefficient (UL) as shown in Fig 3. UL is the sum of top loss coefficient (Ut), back loss coefficient (Ub), and edge loss coefficient (Ue) [7].

$$U_L = U_t + U_b + U_e \tag{1}$$

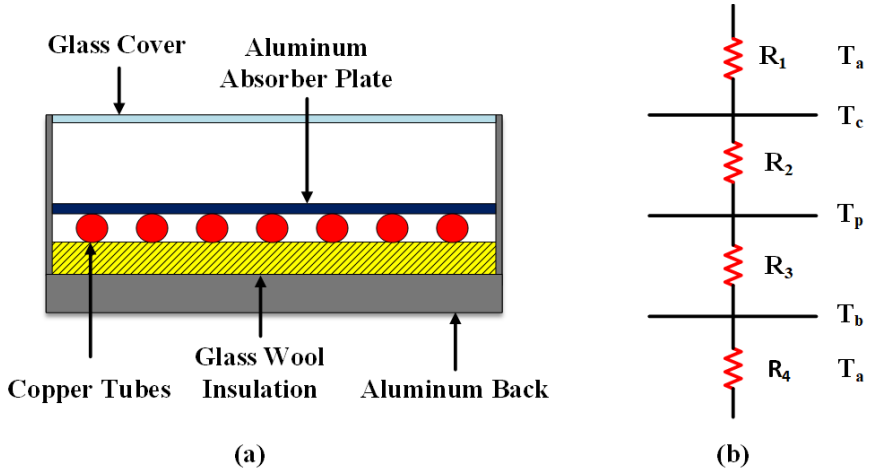

Fig. 3: (a) EFPC side view, (b) Thermal resistance network

Heat transfer coefficients are evaluated to find the overall heat loss coefficient. McAdams formulated Eq. (2) for the calculation of the wind convection coefficient.

$$h_w = 5.7 + 3.8V \tag{2}$$

The following equation is used to calculate the radiative heat transfer coefficient to the sky.

$$h_{\gamma(c-a)} = \sigma\varepsilon_c(T_c^2 + T_s^2)(T_c + T_s) \tag{3}$$

Similarly, the radiative heat transfer coefficient between the glass cover and absorber plate is given by:

$$h_{\gamma(p-c)} = \frac{\sigma(T_c^2 + T_p^2)(T_c + T_p)}{\frac{1}{\varepsilon_c} + \frac{1}{\varepsilon_p} - 1} \tag{4}$$

$$h_{c(p-c)} = Nu\,\frac{k_a}{L} \tag{5}$$

Nusselt number for flow between two parallel plates where height to the spacing ratio between plates is ≥ 12 and tilt angle is up to 70° [7].

$$Nu = 1 + 1.44\left[1 - \frac{1708(sin\,1.8\beta)^{1.6}}{Ra\,cos\beta}\right]\left[1 - \frac{1708}{Ra\,cos\beta}\right]^{+} + \left[\left(\frac{Ra\,cos\beta}{5830}\right)^{\frac{1}{3}} - 1\right]^{+} \tag{6}$$

$$Ra = \frac{g(T_p - T_c)L^3}{T_m\nu\alpha} \tag{7}$$

The total useful energy gain can be found by the product of total incident solar energy and collector heat removal factor (FR). It is given by:

$$Q_u = A_C F_R (S - U_L (T_i - T_a)) \tag{8}$$

Where S represents the total absorbed solar irradiance and Qu represents the total useful thermal energy.
The collector heat removal factor for FPC having copper tubes with serpentine configuration was formulated by Zhang and Lavan in terms of 6 different factors ranging from F1 to F6 [7]. These factors are given in the following equations:

$$F_R = F_1F_3F_5\left[\frac{2F_4}{F_6\,exp\left(-\sqrt{1 - \frac{F_2^2}{F_3}}\right)} - 1\right] \tag{9}$$

$$F_1 = \frac{\kappa}{U_L W} \times \frac{\kappa R(1+\gamma)^2 - 1 - \gamma - \kappa R}{[\kappa R(1+\gamma) - 1]^2 - (\kappa R)^2} \tag{2}$$

$$F_2 = \frac{1}{\kappa R(1+\gamma)^2 - 1 - \gamma - \kappa R} \tag{11}$$

$$F_3 = \frac{\dot{m}C_p}{F_1U_LA_C} \tag{3}$$

$$F_4 = \left(\frac{1 - F_2^2}{F_2^2}\right)^{\frac{1}{2}} \tag{4}$$

$$F_5 = \frac{1}{F_2} + F_4 - 1 \tag{5}$$

$$F_6 = 1 - \frac{1}{F_2} + F_4 \tag{15}$$

$$= \frac{(k\delta U_L)^{\frac{1}{2}}}{sinh\left[(W - D)\left(\frac{U_L}{k\delta}\right)^{\frac{1}{2}}\right]} \tag{16}$$

In Eq. (16), k is plate thermal conductivity, δ is plate thickness, W is the distance between copper tubes and D is the

outside diameter of copper tube.

$$\gamma = -2\cos h\left[(W-D)\left(\frac{U_L}{k\delta}\right)^{\frac{1}{2}}\right] - \frac{DU_L}{\kappa} + F_4 - 1 \quad (17)$$

$$R = \frac{1}{C_b} + \frac{1}{\pi D_i h_{fi}} \quad (18)$$

The fluid convective coefficient is evaluated using the internal flow Eq. (19) by Gnielinski to calculate the Nusselt number [7].

$$Nu = \frac{(f/8)(Re-1000)Pr}{1.07 + 12.7 \times \sqrt{f/8}\left(Pr^{\frac{2}{3}} - 1\right)} \times \left(\frac{\mu}{\mu_w}\right)^n \quad (19)$$

For n, 0.11 and 0.25 are used for heating and cooling applications, respectively. Whereas Darcy friction factor is given by:

$$f = (0.79\ln Re - 1.64)^{-2} \quad (20)$$

Energy Efficiency can be calculated by using collector area, global tilted irradiance, and Eq. (19).

$$\eta = \frac{Q_U}{A_C \times I(\tau\alpha)} \quad (6)$$

3. Results and Discussion

The experimentation is performed on the EFPC system for two days for the location of Islamabad, Pakistan. A data logger is used to acquire data from the system. Later this data was analysed to derive following different conclusions.

3.1. Meteorological Data

Solar energy harvesting is dependent on the solar data and the ambient conditions of the project location. The wind and convection coefficients are dependent on these parameters. Fig 4 shows the variation of solar irradiance, ambient temperature, and wind speed concerning the hour of the day. These figures are based on the data of two test days recorded in Islamabad, dated 31st of December 2020 and 10th of February 2021. The data acquired to illustrate these parameters at 10-second intervals is averaged over the 30-minute interval to achieve consistent results.

On a clear sunny day, there is a gradual increment in irradiance from the sunrise until solar noon. The irradiance keeps on decreasing after noon till the sunset. During a cloudy day, solar irradiance fluctuates depending upon the cloud cover. There is a sudden decrease in irradiance at 01:00 hours on the 31st of December because of the cloudy weather as shown in Fig 3.

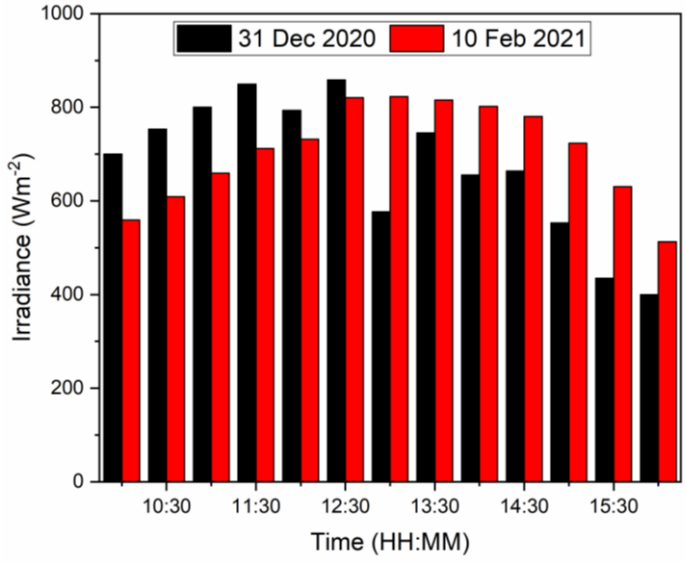

Fig. 4: Variation of weather data with time for two test days: Solar irradiance incident on EFPC at 30° tilt angle.

Fig. 5(a) represents the 30-minute averaged ambient air temperatures of the two test days. At sunrise, ambient temperatures are lower and keep on increasing till dusk. Ambient temperatures may also fluctuate because of rain or cold gusts. The maximum ambient temperature value on the 31st of December 2020 is 17 °C, while it is around 24 °C on the 10th of February 2021. Fig. 5(b) presents wind speed as a function of time.

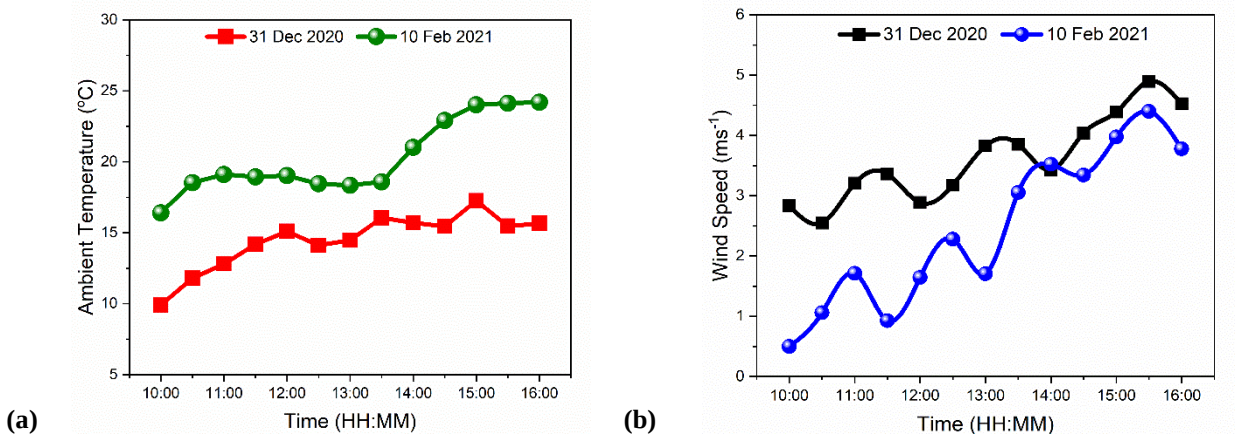

Fig. 5: Variation of weather data with time for two test days: (a) Ambient air temperature vs hour of the day, (b) Wind speed vs hour of the day

3.2. Thermal Efficiency

The thermal efficiency of an EFPC system is evaluated based on several parameters such as ambient temperature, fluid inlet temperature, HTF flow rate, and solar irradiance. The experimental data collected for 2 days with different flow rates for the location of Islamabad under ambient conditions. For the day of 31st of December 2020, the average irradiance is 679.7 Wm-2 with an average ambient temperature equal to 15.3 °C, inlet temperature 31.2 °C and average outlet temperature is 51 °C with HTF flow rate maintained at 3 liters per minute. On the 10th of February 2021, the average ambient temperature, inlet temperature, outlet temperature, and irradiance values are 20.6 °C, 44.3 °C, 59.7 °C, and 718.3 Wm-2, respectively.

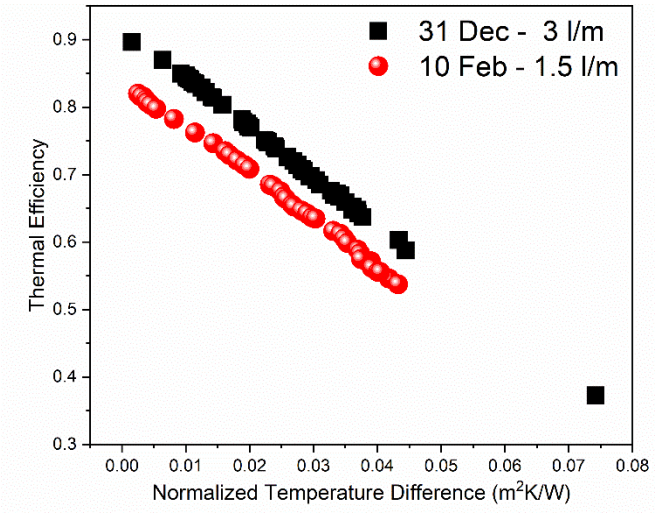

Fig. 6: Thermal efficiency vs NTD for two test days with data points averaged over 5-minute intervals

Normalized temperature difference (NTD) is given by:

$$NTD = \frac{T_i - T_a}{I} \tag{22}$$

Normalized temperature difference is a universal parameter to combine all input variables. Fig 6 represents the normalized temperature difference vs thermal efficiency using Eq. (22) of two different days at two different flow rates. Lower value of normalized temperature difference results in higher thermal efficiency. EFPC system has lower heat losses as compared to recent studies thus achieving higher efficiencies [8].

3.3. Daily Performance Of EFPC

Several tests are performed on the EFPC system on different days during the winter season. Table 1 tabulates the experimental data along with the calculated values of thermal efficiency and useful energy gained by the EFPC. For 2 test days, the thermal efficiency of the EFPC system is given against the solar irradiance, ambient temperatures, the HTF volume flow rate and wind velocity. On a relatively clearer day, the overall thermal efficiency of the EFPC system reached a maximum daily average value of 73.2% with Glycol-Water mixture under 20.0 kPa vacuum. The efficiency of EFPC system is higher than a simple FPC and ETC system [9], [10].

Table 1: Energetic efficiency of experimental test data for 2 different days with the glycol-water mixture

	Date	η	T_i	T_o	T_a	E_{useful}	$E_{absorbed}$	I	V	v_w
	DD.MM.YY	%	°C	°C	°C	$MJm^{-2}hr^{-1}$	$MJm^{-2}hr^{-1}$	Wm^{-2}	$Lmin^{-1}$	ms^{-1}
1	31.12.20	73.2	31.2	51.0	15.3	1.65	2.22	679.7	3	3.75
2	10.02.21	61.0	44.3	59.7	20.6	1.44	2.36	718.3	1.5	2.57

The optimum flow rate for the EFPC system comes out to be 3 litres per minute. Less retention time enables higher flow rate which decreases heat transfer from the absorber to HTF while a lower flow rate does not transfer the total thermal energy from the absorber plate to HTF.

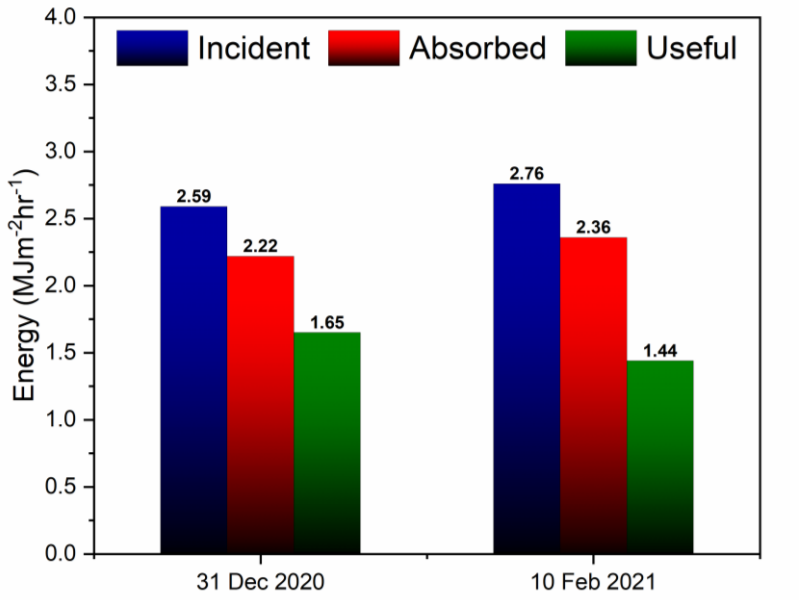

Fig. 7: A comparison between total available solar energy with energy absorbed by EFPCs and useful energy gain by the system for two different test days

In Fig 7, the total solar energy incident on the EFPC collector, total energy absorbed by EFPC after subtracting the optical losses, and total useful energy available at the collector outlet are shown. It is evident that more solar energy is available on the 10th of February 2021, as compared to the 31st of December 2020. The graph shows an increasing trend in useful energy being harvested. Useful energy for the 10th of February 2021, is lower because of the higher value of normalized temperature difference due to lower ambient temperature.

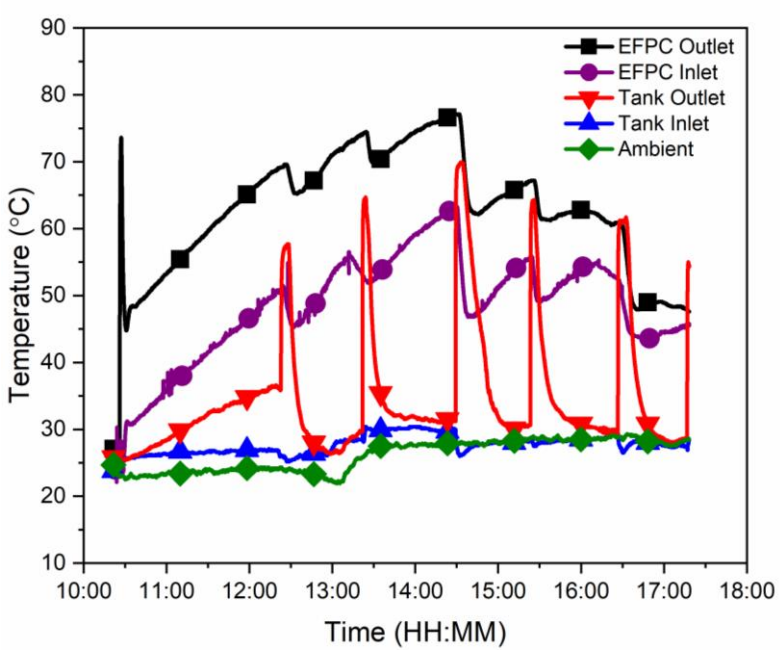

Fig. 8: Variations in temperature at different load points during continuous charging and hourly discharging of EFPC system for the day of the 31st of March 2021

In Fig 8, the first peak in the EFPC outlet contour shows the stagnation temperature of HTF at the instant right after the circulator is turned on. The five peaks in the tank outlet temperature curve starting from 12:30 hours onwards represent the temperature at which hot water is being supplied for household use when the tap is opened. It is important to mention that the freshwater enters the tank at a temperature approximately close to ambient temperature. The temperature at the oulet of the EFPC system is feasible to use it as a source of domestic as well as low temperature industrial usage [11].

4. Conclusion

The experimental research is performed, and the data is analysed to ascertain the feasibility of EFPC system for Islamabad, Pakistan. A low vacuum chamber of 20 kPa is maintained inside the EFPCs compared to the atmospheric pressure of 101.325 kPa. This low vacuum hinders the convective thermal losses between the glass cover and absorber plate. The overall heat loss coefficient of 6.6 $Wm^{-2}K^{-1}$ translates into the average daily thermal efficiency of 73%. This value is far higher than a simple flat plate collector. Thus, an EFPC can store higher thermal energy in the calorifier when the solar irradiance is low. This suggests the use of EFPC for domestic as well as industrial applications.

References

[1] International Energy Agency, "Key World Energy Statistics 2020," Paris, 2020. [Online]. Available: https://www.oecd-ilibrary.org/energy/key-world-energy-statistics-2020_295f00f5-en.

[2] M. Asif, "Sustainable energy options for Pakistan," *Renew. Sustain. Energy Rev.*, vol. 13, no. 4, pp. 903–909, May 2009, doi: 10.1016/j.rser.2008.04.001.

[3] Alternative Energy Development Board, "Power Policy: Alternative and Renewable Energy, 2019," Islamabad, 2020. [Online]. Available: https://www.aedb.org/ae-policies/draft-are-policy-2019.

[4] H. Dagdougui, A. Ouammi, M. Robba, and R. Sacile, "Thermal analysis and performance optimization of a solar water heater flat plate collector: Application to Tétouan (Morocco)," *Renew. Sustain. Energy Rev.*, vol. 15, no. 1, pp. 630–638, Jan. 2011, doi: 10.1016/j.rser.2010.09.010.

[5] G. S. F. Shire, R. W. Moss, P. Henshall, F. Arya, P. C. Eames, and T. Hyde, "Development of an Efficient Low- and Medium-Temperature Vacuum Flat-Plate Solar Thermal Collector," in *Renewable Energy in the Service of Mankind Vol II*, vol. II, Cham: Springer International Publishing, 2016, pp. 859–866.

[6] M. Hazami, S. Kooli, N. Naili, and A. Farhat, "Long-term performances prediction of an evacuated tube solar

water heating system used for single-family households under typical Nord-African climate (Tunisia)," *Sol. Energy*, vol. 94, pp. 283–298, 2013, doi: 10.1016/j.solener.2013.05.020.
[7] J. A. Duffie and W. A. Beckman, "Solar Engineering of Thermal Systems," p. 936, 2013.
[8] H. J. Jouybari, M. E. Nimvari, and S. Saedodin, "Thermal performance evaluation of a nanofluid-based flat-plate solar collector: An experimental study and analytical modeling," *J. Therm. Anal. Calorim.*, vol. 137, no. 5, pp. 1757–1774, 2019, doi: 10.1007/s10973-019-08077-z.
[9] E. Shojaeizadeh, F. Veysi, T. Yousefi, and F. Davodi, "An experimental investigation on the efficiency of a Flat-plate solar collector with binary working fluid: A case study of propylene glycol (PG)–water," *Exp. Therm. Fluid Sci.*, vol. 53, pp. 218–226, Feb. 2014, doi: 10.1016/j.expthermflusci.2013.12.011.
[10] L. M. Ayompe and A. Duffy, "Thermal performance analysis of a solar water heating system with heat pipe evacuated tube collector using data from a field trial," *Sol. Energy*, vol. 90, pp. 17–28, Apr. 2013, doi: 10.1016/j.solener.2013.01.001.
[11] E. Fuentes, L. Arce, and J. Salom, "A review of domestic hot water consumption profiles for application in systems and buildings energy performance analysis," *Renew. Sustain. Energy Rev.*, vol. 81, pp. 1530–1547, Jan. 2018, doi: 10.1016/J.RSER.2017.05.229.

Nomenclature

Nomenclature		Abbreviations	
A_C	Collector Area, m^2	AEDB	Alternative Energy Development Board
C_p	Specific heat at constant pressure, $Jkg^{-1}K^{-1}$	BP	British Petroleum
D_i	Tube inside diameter, m	CFD	Computational Fluid Dynamics
D_o	Copper tube outside diameter, m	CSP	Concentrated Solar Power
f	Darcy friction factor	EFPC	Evacuated Flat Plate Collector
G_T	Absorbed global tilted irradiance, Wm^{-2}	EN	European Standards
h_c	Convection heat transfer coefficient, $Wm^{-2}K^{-1}$	ETC	Evacuated Tube Collector
h_{fi}	Fluid to tube heat transfer coefficient, $Wm^{-2}K^{-1}$	ETFE	Ethylene Tetrafluoroethylene
h_r	Radiation heat transfer coefficient, $Wm^{-2}K^{-1}$	FEM	Finite Element Methods
h_w	Wind convection coefficient, $Wm^{-2}K^{-1}$	FPC	Flat Plate Collector
I	Incident Solar Irradiance, Wm^{-2}	GHI	Global Horizontal Irradiance
k_a	Thermal conductivity of air, $Wm^{-1}K^{-1}$	GTI	Global Tilted Irradiance
k_b	Thermal conductivity of back insulation, $Wm^{-1}K^{-1}$	GW	Giga Watt
L	Distance between tubes, m	HTF	Heat Transfer Fluid
$\dot{m}$	Mass flow rate, kgs^{-1}	IEA	International Energy Agency
Nu	Nusselt number	W	Distance between copper tubes, m
P_g	Gauge Pressure, kPa		
Pr	Prandtl number		
Q_u	Useful Energy, J		
Ra	Raleigh number		
S	Absorbed Solar irradiance, Wm^{-2}		
U_b	Back loss coefficient, $Wm^{-2}K^{-1}$		
U_e	Edge loss coefficient, $Wm^{-2}K^{-1}$		
U_L	Overall collector heat loss coefficient, $Wm^{-2}K^{-1}$		
U_t	Top loss coefficient, $Wm^{-2}K^{-1}$		
v_w	Wind velocity, ms^{-1}		
V	Volume flow rate, $Lmin^{-1}$		

Greek Symbols			
μ	Dynamic Viscosity	H	Efficiency
α	Absorptivity	N	Kinematic Viscosity
β	Tilt Angle	Σ	Stefan-Boltzmann Constant, 5.67×10^{-8} $Wm^{-2}K^{-4}$
Δ	Thickness	T	Transmissivity
ε	Emissivity		